JACS
JOURNAL OF THE AMERICAN CHEMICAL SOCIETY

Article

pubs.acs.org/JACS

Simultaneous Detection of ATP and GTP by Covalently Linked Fluorescent Ribonucleopeptide Sensors

Shun Nakano,[†] Masatora Fukuda,[†] Tomoki Tamura,[†] Reiko Sakaguchi,[†] Eiji Nakata,[†,‡] and Takashi Morii*[,†,‡]

[†]Institute of Advanced Energy, Kyoto University, and [‡]CREST, JST, Uji, Kyoto 611-0011, Japan

Supporting Information

ABSTRACT: A noncovalent RNA complex embedding an aptamer function and a fluorophore-labeled peptide affords a fluorescent ribonucleopeptide (RNP) framework for constructing fluorescent sensors. By taking an advantage of the noncovalent properties of the RNP complex, the ligand-binding and fluorescence characteristics of the fluorescent RNP can be independently tuned by taking advantage of the nature of the RNA and peptide subunits, respectively. Fluorescent sensors tailored for given measurement conditions, such as a detection wavelength and a detection concentration range for a ligand of interest can be easily identified by screening of fluorescent RNP libraries. The noncovalent configuration of a RNP becomes a disadvantage when the sensor is to be utilized at very low concentrations or when multiple sensors are applied to the same solution. Here, we report a strategy to convert a fluorescent RNP sensor in the noncovalent configuration into a covalently linked stable fluorescent RNP sensor. This covalently linked fluorescent RNP sensor enabled ligand detection at a low sensor concentration, even in cell extracts. Furthermore, application of both ATP and GTP sensors enabled simultaneous detection of ATP and GTP by monitoring each wavelength corresponding to the respective sensor. Importantly, when a fluorescein-modified ATP sensor and a pyrene-modified GTP sensor were co-incubated in the same solution, the ATP sensor responded at 535 nm only to changes in the concentration of ATP, whereas the GTP sensor detected GTP at 390 nm without any effect on the ATP sensor. Finally, simultaneous monitoring by these sensors enabled real-time measurement of adenosine deaminase enzyme reactions.

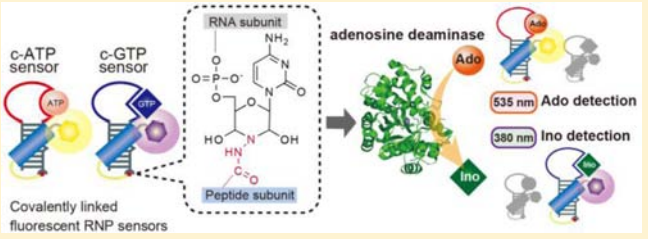

INTRODUCTION

Fluorescent biosensors that are able to detect specific ligands with high sensitivity have been developed from macromolecular receptors.[1] The first step in the construction of fluorescent biosensors often starts with the search for natural receptors that possess ideal affinity and selectivity for the target molecule. Otherwise, a novel receptor with necessary affinity and selectivity has to be constructed. For conversion of receptors into fluorescent biosensors, mutants of the receptor are designed by examination of the position of mutation in which substrate binding is effectively converted into optical signals based on the 3-dimensional structural information of the receptors.[2] The sensor that has the desired substrate-binding and fluorescent properties is then constructed by chemical modification of the fluorophore to the mutant, followed by evaluation of its function as a sensor. Fluorescent biosensors have been developed by various methods based on this general concept. However, it is still difficult to predict whether a receptor that is modified by a fluorophore at a specific position could effectively respond to a ligand of interest at the desired fluorescent wavelength, even based on detailed 3-dimensional structural information of the receptor. Indeed, many designed sensors do not necessarily show desired fluorescent responses. Moreover, modification of the receptor with a fluorophore often results in a decrease or loss of the affinity or selectivity to the substrate.

We previously reported a candidate fluorescent sensor that utilized a ribonucleopeptide (RNP) framework.[3] In this prior study, an RNA-derived RNP library was prepared by introducing a randomized nucleotide region as a ligand-binding domain adjacent to the Rev Responsive Element (RRE) RNA segment of an RRE-Rev peptide complex[4] in a structure-based manner. An in vitro selection method[5] was applied to the RNA-based RNP library to afford a series of RNP receptors for given targets.[3a−e] In the second step, substitution of the Rev peptide by the fluorophore-modified Rev peptide of the selected RNP receptor afforded a fluorescent RNP complex that showed fluorescence intensity changes upon binding to the target molecule without loss of affinity or selectivity of the parent RNP receptor. The RNA subunits obtained by the in vitro selection of the RNP library usually display many kinds of sequences, even sharing the same consensus sequence. Because each RNP shows a different affinity to the target molecule, these RNA subunits are used as a library that binds to the target with various affinities and structures. On the other hand, a library of fluorophore-modified Rev peptides is easily

Received: October 3, 2012
Published: February 1, 2013

   dx.doi.org/10.1021/ja3097652 | J. Am. Chem. Soc. 2013, 135, 3465−3473

constructed by modifying the Rev peptide with fluorophores that have a variety of excitation and emission wavelengths. By taking advantage of the characteristic of the RNP as a noncovalent complex, combinations of the RNA subunit library and the fluorescent Rev library afford a pool of fluorescent RNPs with various characters. From the fluorescent RNP library, fluorescent RNP sensors for targets, such as ATP,[3c,d] phosphotyrosine residues in defined amino acid sequences,[3e] and dopamine,[3h] were obtained that respond at detection or excitation wavelengths and have ligand affinities and ligand concentration ranges of interest. For example, ATP sensors were obtained with the dissociation constants ranging from 2.2 to 156 μM, and with the detection wavelengths from 390 to 670 nm.

The noncovalent RNP sensor complex is also characterized by a modular structure in which the ligand-binding RNA module and the fluorophore-labeled Rev peptide and RRE RNA complex, a sensing module, are connected through a spacer RNA. Modular design of fluorescent sensors is therefore possible by using an existing RNA aptamer as the sensing module. A GTP-binding RNA aptamer isolated by in vitro selection is utilized as the ligand-binding module of the RNP sensor by fusing it to RRE RNA, and successive complexation with the fluorophore-labeled Rev peptide affords a fluorescent GTP sensor.[3g,i] Almost all RNP sensors exhibited fluorescence quenching upon RNP complex formation and restored their intrinsic fluorescence after substrate binding.[3c−i]

This stepwise strategy conveniently provides fluorescent RNP sensors with various detection wavelengths and detection ranges for a given target by combination of RNP aptamers and fluorophore-modified peptides, but the noncovalent configuration becomes a disadvantage for practical measurements, for instance, when the sensor concentration is reduced. Previously reported bimolecular sensors, such as signaling aptamers[6] and aptamer sensors noncovalently embedded with a fluorophore,[7] would face the same situation. In addition, simultaneous application of multiple noncovalent sensors that consist of the same Rev/RRE scaffold would suffer from exchanges between the subunits. Therefore, this system needs an improvement for its orthogonal usage. Furthermore, development of a strategy to construct stable fluorescent biosensors will facilitate simultaneous detection of two or more cellular signaling molecules at different detection wavelengths. Such a set of biosensors will be quite useful for understanding cellular signaling pathways, even when applied to cellular extracts in vitro.

An effective method to overcome the disadvantages of the noncovalent character of receptors has been reported for antibody engineering,[8] such as in the modification of immunoglobulin Fv fragments that form as a result of the noncovalent complexing of heterodimers of the heavy-chain variable domain (V_H) and the light-chain variable domain (V_L).[9] The stability of Fv fragments was increased by covalently linking each chain with a disulfide bond[10] or connecting V_H and V_L proteins with a flexible linker peptide to form a single-chain Fv molecule.[11] This covalent linking strategy would also be applicable to the modular RNP sensor. A covalent linkage between the RNA and the peptide subunits is expected not only to enhance the stability of the RNP complex, but also to prevent the exchange of the subunits between multiple RNP sensors.

Here, we report the synthesis of stable fluorescent RNP sensors by covalently linking the RNA and fluorophore-modified Rev peptide subunits and demonstrate that the covalent RNP sensors are capable of detecting multiple ligands simultaneously in the same solution at different wavelengths with low sensor concentrations, even in cellular extracts.

RESULTS AND DISCUSSION

Construction of Covalently Linked Fluorescent RNP Sensors. Noncovalent fluorescent RNP sensors for nucleotide triphosphates were constructed as previously reported.[3c] To construct a stable fluorescent RNP sensor, the 3′-terminal of RNA subunit and the C-terminal of Rev peptide were covalently tethered by a hydrazone bond formation[12] (Figure 1). This reaction has been utilized as an immobilization method

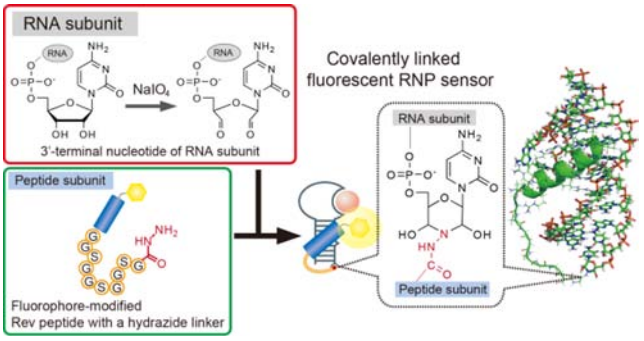

Figure 1. Schematic illustration of the construction of covalently linked fluorescent RNP sensor. 3′-Ribose of the RNA subunit was converted to 3′-dialdehyde by treating with sodium periodate. A flexible peptide linker (GGSGGSGGSG) with a carboxyhydrazine was introduced at the C-terminal of the fluorophore-modified Rev peptide. A covalently linked fluorescent RNP sensor was synthesized through a coupling of these modified RNA and peptide subunits via hydrazone bond formation.

of nucleic acids or proteins to solid supports[12a,e,h] or as a cross-linking method of nucleic acids and/or proteins.[12f] The RNA subunit of ATP-binding RNP was treated with sodium periodate to form a 3′-dialdehyde group. A flexible linker with ten amino acid residues (GGSGGSGGSG) was introduced at the C-terminal of the Rev peptide, and a hydrazine group was introduced to the C-terminal. The length of the linker GGSGGSGGSG was determined by reference to the 3-dimensional structure of the complex of the Rev peptide and RRE RNA (Figure S1).[4] A linker with seven amino acid residues (GGSGGSG) seemed too short to tether the Rev peptide to RRE RNA (Figure S1a). No obvious steric hindrance was observed for the Rev/RRE complexes with linker over seven amino acid residues (Figure S1b,c). Therefore, the linker with ten amino acid residues was utilized for the covalent linkage between the C-terminal of Rev peptide and the 3′-end of RRE RNA (Figure S1c).

The noncovalent complexes of fluorescent RNP sensors for ATP and GTP were converted to covalently linked RNPs to confirm the above strategy. Among the ATP-binding RNP receptors with various affinity to ATP selected from the RNP library,[3c] A26 RNP was chosen as a representative RNP because A26 RNP binds to ATP and ATP-derivatives including Ado with moderate affinities,[3c,f] which is ideal for the measurement of the changes in ATP concentration to reduce the interference from the ATP endogenous to the cellular extracts. In addition, A26 RNP shows measurable changes in fluorescence intensities upon binding to the targets with many types of fluorophore (Pyr, NBD, Cy5, etc.).[3c] In a similar manner, G23 RNP was

dx.doi.org/10.1021/ja3097652 | J. Am. Chem. Soc. 2013, 135, 3465−3473

chosen from the selected GTP-binding RNP receptors[3c] because of its moderate affinity to GTP and fluorescent response. Purified RNA subunits of these RNPs, A26 RNA and G23 RNA, were treated with freshly prepared sodium periodate to modify the 3′-terminal ribose to 3′-dialdehyde by periodate oxidation. The peptide subunit for the covalent linkage was synthesized by introducing a peptide linker (GGSGGSGGSG) at the C-terminus, coupling a fluorophore to the N-terminal of the Rev peptide, and derivatized to hydrazide by hydrazine treatment of the resin. 5-Carboxyfluorescein, 1-pyrenesulfonyl chloride, and Cy5 were conjugated to the N-terminal amino group of the Rev peptide to give 5FAM-Rev-HZ, Pyr-Rev-HZ, and Cy5-Rev-HZ, respectively. These peptides were purified by HPLC and characterized by MALDI-TOF mass spectrometry.

Subsequently, the modified RNA and peptide subunits were covalently linked together. Coupling reactions of A26 RNA 3′-dialdehyde and 5FAM-Rev-HZ or G23 RNA 3′-dialdehyde and Pyr-Rev-HZ were performed in sodium acetate buffer (pH 5.2) at 37 °C. The resulting covalently linked RNP complex was purified by phenol-chloroform extraction, ethanol precipitation, and denaturing PAGE to remove the unreacted RNA and peptide. The isolated yields of covalently linked RNPs of A26 RNA with 5FAM-Rev-HZ (c-A26/5FAM-Rev) and G23 RNA with Pyr-Rev-HZ (c-G23/Py-Rev) were 36% and 32%, respectively. The purities of the covalently linked RNP sensors were checked by denaturing PAGE (Figure S2). After PAGE purification and isolation, c-A26/5FAM-Rev and c-G23/Pyr-Rev were characterized by MALDI-TOF mass spectroscopy. c-An16/Cy5-Rev and c-G23/5FAM-Rev were prepared using the same procedure. The coupling yields for the native and denaturing conditions for the RNP complex were similar to each other (Figure S3), indicating that the formation of RNP is not a prerequisite for the reaction.

Fluorescent Responses of the Covalent RNP Complexes. The fluorescence responses of the covalently linked ATP sensor (c-A26/5FAM-Rev), the covalently linked GTP sensor (c-G23/Pyr-Rev), and each corresponding noncovalent derivative (i.e., A26/5FAM-Rev and G23/Pyr-Rev, respectively) were evaluated in the presence of increasing concentrations of ATP or GTP (Figure 2). Relative fluorescence intensities (I/I_0) of ATP sensors were calculated by dividing the fluorescence intensity in the presence (I) of ATP by the fluorescence intensity in the absence (I_0) of ATP (Figure 2). Relative fluorescence intensities were plotted against the ATP concentration to calculate the dissociation constant (K_D) for the complex between the RNP sensor and ATP. The saturation value of the change in relative fluorescence intensity was found to be 1.6 for c-A26/5FAM-Rev (100 nM), which was similar to the value of 1.7 for A26/5FAM-Rev (1000 nM). K_D values for the ATP complexes of c-A26/5FAM-Rev (100 nM) and A26/5FAM-Rev (1000 nM) were 6.3 and 13.4 μM, respectively (Figure 2a,b). The binding affinity of covalently linked c-A26/5FAM-Rev was higher than that of noncovalent A26/5FAM-Rev.

The K_D value of the Rev-RRE complex has been shown to be a few nanomolar at similar buffer conditions to those used in this study.[13] The covalently linked sensor c-A26/5FAM-Rev provided distinct fluorescent responses, even at 1 nM (Figure 2a). On the other hand, the noncovalent sensor A26/5FAM-Rev exhibited almost no fluorescent response when the RNP concentration was reduced to 100 nM (Figure 2b), indicating that the noncovalent RNP complex was mostly dissociated into each subunit. Furthermore, the fluorescence response of the

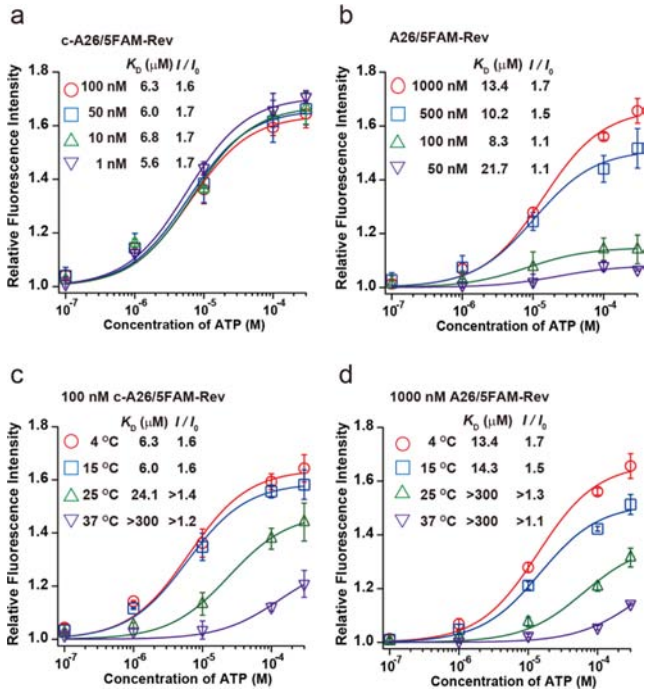

Figure 2. Saturation curves for the relative fluorescence intensity changes of c-A26/5FAM-Rev and A26/5FAM-Rev by titration with ATP in a buffer containing 10 mM Tris-HCl (pH 7.6), 100 mM NaCl, 10 mM $MgCl_2$, and 0.005% Tween 20. (a) Titration of the ATP-binding fluorescent RNP complexes c-A26/5FAM-Rev (1 nM, purple reverse triangles; 10 nM, green triangles; 50 nM, blue squares; 100 nM, red circles) with ATP at 4 °C and (b) A26/5FAM-Rev (50 nM, purple reverse triangles; 100 nM, green triangles; 500 nM, blue squares; 1000 nM, red circles) with ATP at 4 °C are shown. (c) Titration profiles of the ATP-binding fluorescent RNP complexes c-A26/5FAM-Rev and (d) A26/5FAM-Rev with ATP at different temperatures (4 °C, red circles; 15 °C, blue squares; 25 °C, green triangles; 37 °C, purple reverse triangles) are shown. The dissociation constant (K_D) and the maximum relative fluorescence intensity for the ATP complex of each RNP are shown in the inset.

covalently linked sensor c-A26/5FAM-Rev showed higher tolerance to increasing temperatures, even at a sensor concentration of 100 nM (Figure 2c), than that of A26/5FAM-Rev (1000 nM; Figure 2d).

The covalently linked GTP sensor c-G23/Pyr-Rev showed a higher affinity to GTP than that of the noncovalent sensor G23/Pyr-Rev (Figure 3a). The I/I_0 value for c-G23/Pyr-Rev and GTP at the saturation was 3.1, which was significantly higher than that of the parent noncovalent GTP sensor G23/Pyr-Rev (1.8). Again, the covalently linked sensor c-G23/Pyr-Rev showed higher tolerance to increasing temperatures (Figure 3b) than that of G23/Pyr-Rev (Figure 3c).

These results indicated that the noncovalent RNP sensors for ATP or GTP were converted to a covalently linked RNP sensor without diminishing sensing functions for ATP or GTP, respectively. The covalently linked RNP sensor exhibited much higher stability at low concentrations and maintained the fluorescence response of individual RNP sensors.

Simultaneous Detection of ATP and GTP by Fluorescent RNP Sensors. Because the fluorophore-modified Rev peptide binds to a common RRE RNA sequence, a unique noncovalent RNP sensor must be applied for each separate sample solution to reduce the possible exchange between different subunits of multiple RNP species. In contrast, the

dx.doi.org/10.1021/ja3097652 | J. Am. Chem. Soc. 2013, 135, 3465−3473

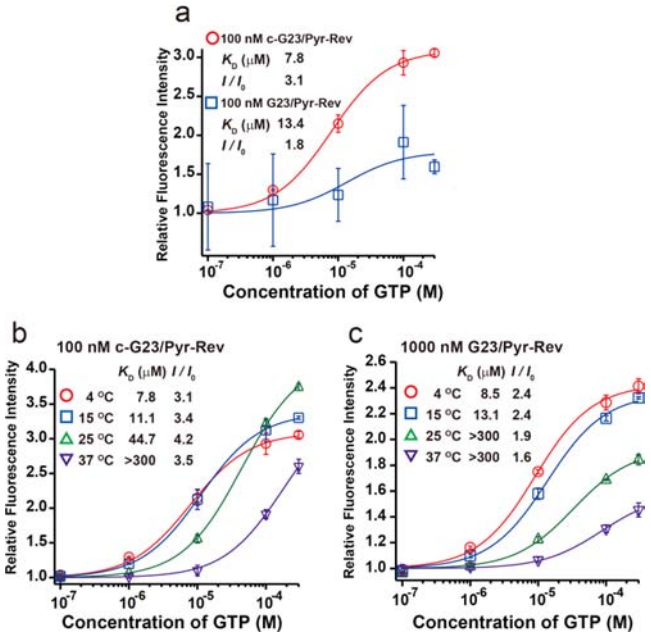

Figure 3. (a) Saturation curves for the relative fluorescence intensity changes of c-G23/Pyr-Rev (100 nM, red circles) and G23/Pyr-Rev (100 nM, blue squares) by titration with GTP in a buffer containing 10 mM Tris-HCl (pH 7.6), 100 mM NaCl, 10 mM $MgCl_2$, and 0.005% Tween 20 at 4 °C. (b) Titration profiles of c-G23/Pyr-Rev and (c) G23/Pyr-Rev with GTP at different temperatures (4 °C, red circles; 15 °C, blue squares; 25 °C, green triangles; 37 °C, purple reverse triangles) are shown. The dissociation constant (K_D) and the maximum relative fluorescence intensity for the GTP complex of each RNP are shown in the inset.

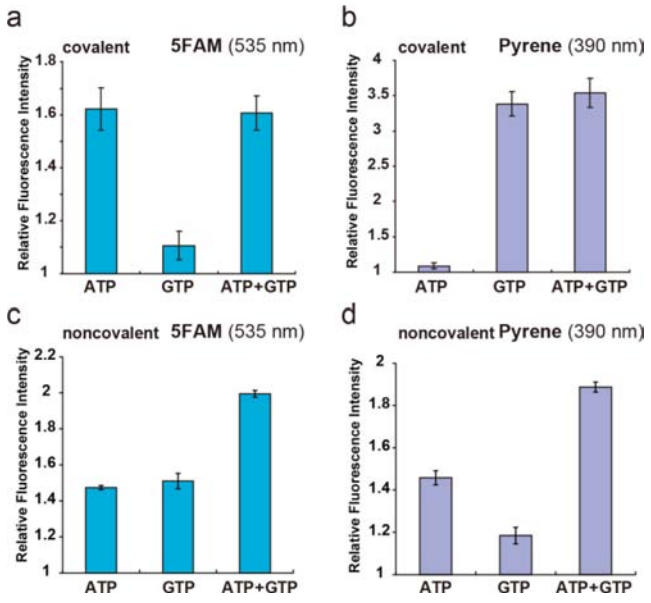

Figure 4. (a,b) Simultaneous detection of ATP and GTP by covalently linked ATP and GTP sensors at different wavelengths in the same solution. A solution containing both the ATP sensor c-A26/5FAM-Rev (100 nM) and the GTP sensor c-G23/Pyr-Rev (100 nM) in the presence of 100 μM ATP and/or 100 μM GTP was measured at (a) 535 nm or at (b) 390 nm at 4 °C to selectively detect ATP or GTP. (c,d) Fluorescence responses of noncovalent ATP and GTP sensors at different wavelengths in the same solution in the presence of ATP, GTP, or both ATP and GTP. A solution containing both the ATP sensor A26/5FAM-Rev (1000 nM) and the GTP sensor G23/Pyr-Rev (1000 nM) in the presence of 100 μM ATP and/or 100 μM GTP was measured at (c) 535 nm or at (d) 390 nm at 4 °C under the mixing condition.

covalently linked RNP sensor forms an intramolecular complex that prevents such an exchange between the subunits, even when several types of RNP sensors coexist in the solution.

To test this, the covalently linked sensors c-A26/5FAM-Rev and c-G23/Pyr-Rev were applied to monitor the concentrations of ATP and GTP in the same solution at different wavelengths. The ATP sensor c-A26/5FAM-Rev shares the same consensus sequence with the ATP-binding RNP A26/5FAM-Rev, which selectively binds ATP over GTP.[3f] The parent RNP of the covalent GTP sensor, G23/Pyr-Rev, has been shown to distinguish GTP from ATP.[3c] When monitored at 535 nm, the ATP sensor c-A26/5FAM-Rev responded to concentration changes in ATP, but not to changes in the concentration of GTP (Figure 4a), and showed a similar response that was observed in the absence of the GTP sensor c-G23/Pyr-Rev (Figure 2a). Similarly, the GTP sensor c-G23/Pyr-Rev specifically detected GTP at 390 nm without any interference from ATP and the ATP sensor c-A26/5FAM-Rev in the same solution (Figure 4b). In contrast, the solution containing both the noncovalent sensors A26/5FAM-Rev and G23/Pyr-Rev showed fluorescence responses to both ATP and GTP at the detection wavelengths of 5FAM and Pyr (Figure 4c,d). This result suggests that exchange of 5FAM-Rev and Pyr-Rev has occurred for the noncovalent RNP sensors in the solution. These results indicate that ATP and GTP in the same solution are specifically detected by c-A26/5FAM-Rev and c-G23/Pyr-Rev, respectively, in the presence of other substrate and/or the other sensor.

The combination of an appropriate RNA subunit of an ATP- or GTP-binding RNP and a fluorophore-modified Rev peptide afforded a set of covalently linked fluorescent sensors for the simultaneous detection of ATP and GTP. By using the RNA subunit An16 derived from an ATP-binding RNP[3a] and a Cy5-modified Rev peptide, the covalently linked RNP sensor c-An16/Cy5-Rev, which responded to ATP with a K_D lower than 200 nM at 670 nm, was obtained (Figure S4a). Likewise, covalent linking of G23 RNA with a fluorescein-labeled Rev peptide (5FAM-Rev) afforded c-G23/5FAM-Rev, which detected GTP at 535 nm with a K_D of 2.0 μM (Figure S4b). When the two sensors exist in the same solution, the ATP sensor c-An16/Cy5-Rev responded at 670 nm to ATP with a similar K_D value determined under the single sensor condition (K_D < 200 nM) (Figures S4c and S4e). Furthermore, ATP titration in the presence of equal amounts of GTP did not show significant interference of GTP (K_D for ATP < 200 nM) (Figure S4 c and e). Similarly, the binding ability of GTP sensor c-G23/5FAM-Rev to GTP was not interfered in the presence of ATP sensor (K_D = 2.0 μM) and ATP (K_D = 2.3 μM). Thus, the two sensors c-An16/Cy5-Rev and c-G23/5FAM-Rev were amenable to simultaneous measurement of their respective ligands at different detection wavelengths in the same solution.

These results demonstrate that simultaneous detection of multiple ligands is possible by applying covalently linked RNP sensors that sense their respective ligands at different detection wavelengths. In addition, a variety of sensors that respond at the target concentration range with the desired detection wavelength would be prepared by the combination of an appropriate RNA subunit and a fluorophore-labeled Rev peptide.

dx.doi.org/10.1021/ja3097652 | J. Am. Chem. Soc. 2013, 135, 3465−3473

Simultaneous Detection of a Substrate and a Product in an Enzymatic Reaction by Covalently Linked Fluorescent RNP Sensors. Covalent RNP sensors were next applied for real-time monitoring of an enzymatic conversion of adenosine (Ado) to inosine (Ino) catalyzed by adenosine deaminase (ADA; Figure 5a).[14] In order to monitor the concentration changes of Ado and Ino in the same solution at different wavelengths, c-A26/5FAM-Rev and c-G23/Pyr-Rev were utilized. ATP sensors can recognize Ado with similar affinity and fluorescence response to ATP[3f] (Figure S5). Covalently linked c-G23/Pyr-Rev was used for Ino detection in this assay because the parent G23/Pyr-Rev showed moderate affinity and sufficient relative fluorescence intensity changes to Ino, and importantly, G23/Pyr-Rev possessed distinct selectivity to Ino over Ado in our GTP-binding RNPs.[3c] Titration analyses for each sensor revealed that c-A26/5FAM-Rev responded specifically to changes in Ado concentrations at 535 nm, with a K_D of 11.4 μM (Figure 5b), while c-G23/Pyr-Rev monitored Ino concentrations at 380 nm, with a K_D of 108 μM (Figure 5c). The GTP sensor c-G23/Pyr-Rev showed much lower affinity to Ino than that to GTP, but exhibited a distinctive selectivity to Ino over Ado (Figure 5c).

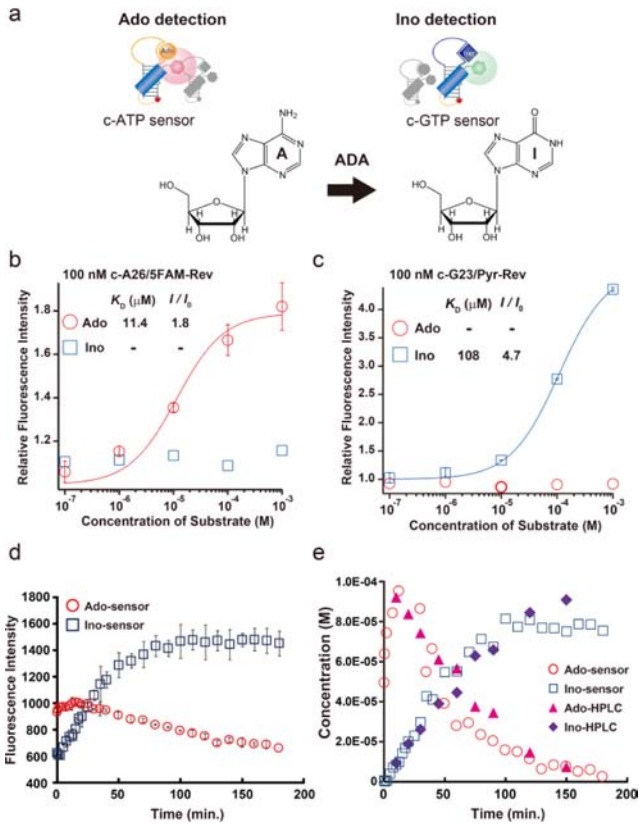

Figure 5. (a) Conversion of adenosine (Ado) to inosine (Ino) catalyzed by adenosine deaminase (ADA). The covalently linked RNP sensors for ATP and GTP responded to changes in the concentrations of Ado and Ino, respectively. Saturation curves for the relative fluorescence intensity changes of c-A26/5FAM-Rev and c-G23/Pyr-Rev by Ado and Ino in a buffer containing 10 mM Tris-HCl (pH 7.6), 100 mM NaCl, 10 mM $MgCl_2$, and 0.005% Tween 20 at 15 °C are shown. Titration analyses were performed for (b) c-A26/5FAM-Rev (100 nM) and (c) c-G23/Pyr-Rev (100 nM) with Ado (circles) or Ino (squares). Observed equilibrium dissociation constants (K_D) and the maximum relative fluorescence intensity change (I/I_0) are shown in the inset. (d) Time-dependent changes in the fluorescence intensities of the covalent sensors c-A26/5FAM-Rev (circles) and c-G23/Pyr-Rev (squares), which monitored the conversion of Ado to Ino by ADA. (e) Overlay plots of time-dependent changes in the concentrations of Ado and Ino were quantified by the covalently linked RNP sensors c-A26/5FAM-Rev and c-G23/Pyr-Rev and by HPLC. HPLC quantification data were converted to the corresponding concentrations of Ado (pink filled triangles) and Ino (purple filled diamonds). Fluorescence intensity changes of c-RNP sensors were converted to changes in the concentrations of Ado (red open circles) and Ino (blue open squares) using their respective titration curves (Figure S8).

Next, the covalent sensors c-A26/5FAM-Rev and c-G23/Pyr-Rev were mixed in a solution containing Ado (100 μM). After incubation for 30 min at 15 °C, ADA (0.1 mU) was added to the solution to start the reaction. When monitored at 535 nm, the fluorescence intensity of the ATP sensor c-A26/5FAM-Rev decreased with the reaction time, indicating that c-A26/5FAM-Rev responded to decreases in Ado concentrations (Figure 5d). Measurement of the fluorescence intensity of c-G23/Pyr-Rev at 380 nm showed a gradual increase with incubation time, which corresponded to the time-dependent production of Ino. The reaction of ADA was also evaluated by HPLC to quantitatively assess the consumption of Ado and the production of Ino (Figures S6 and S7). Quantification of the peak area of each nucleoside (i.e., Ado and Ino) in the enzymatic reaction afforded actual changes in the concentrations of each nucleoside. The fluorescence intensity changes monitored by the RNP sensors were also converted to time-dependent concentration changes for Ado and Ino using the quantitative titration curves (Figure S8).

These time-course profiles were overlaid to compare changes in the concentrations of Ado and Ino as obtained by HPLC and RNP sensors (Figure 5e). Both profiles for changes in Ado concentrations obtained by the RNP sensor and the HPLC analysis were almost identical, other than the initial phase (up to 30 min) of the enzymatic reaction. In addition, the time-course profile for the formation of Ino monitored by c-G23/Pyr-Rev was also almost identical to the profile obtained by quantitative HPLC analysis. Therefore, time-dependent changes in the concentrations of Ado and Ino in the ADA reaction were simultaneously quantified using the covalent sensors c-A26/5FAM-Rev and c-G23/Pyr-Rev, respectively, across the range of times and substrate concentrations studied.

Thus, this covalent strategy for generating RNP sensors afforded multiple fluorescent detecting system that were suitable for monitoring the conversion process within a given concentration range. Further practical employment of the covalent RNP sensors including the real-time monitoring of other enzymatic reaction process, will be promised by preparation of RNA subunit with various characteristics such as the specificity and/or selectivity toward ligands.

Enhancement of the Stability of Covalent RNP Sensors in Cellular Extracts. The covalent linkage of RNP subunits increased the thermodynamic stability of RNP. At the same time, such a modification was expected to enhance the tolerance of RNP to degradation in cellular culture media. To evaluate the stability of the covalent RNP sensor in the cellular media, the covalent ATP sensor was titrated by ATP in HeLa cell extracts at ambient temperature. An ATP-binding RNP receptor (A26/Rev) with a moderate K_D value[3a] was utilized for the titration experiments to reduce the interference from the ATP endogenous to the cellular extracts (Figure 6a).

The noncovalent A26/5FAM-Rev complex showed higher stability than A26RNA alone in the cell extract at 4 °C,[3e] but an

dx.doi.org/10.1021/ja3097652 | J. Am. Chem. Soc. 2013, 135, 3465−3473

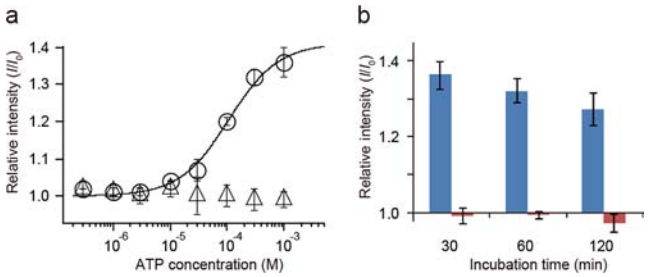

Figure 6. (a) Titration analyses of noncovalent A26/5FAM-Rev (200 nM, open triangles) and covalent c-A26/5FAM-Rev (200 nM, open circles) following addition of ATP in HeLa cell extracts upon incubation for 30 min at ambient temperature. (b) Evaluation of the stabilities of A26/5FAM-Rev (red bars) and c-A26/5FAM-Rev (blue bars) in HeLa cell extracts. Each sensor was mixed with ATP (1 mM) and incubated in HeLa cell extracts at ambient temperature for the indicated times. The change in relative fluorescent intensity was measured by a Wallac ARVOsx 1420 multilabel counter (Perkin-Elmer).

incubation of A26/5FAM-Rev in HeLa cell extracts at ambient temperature for 30 min led to a complete loss of the fluorescence response to the ATP titration (Figure 6a). In contrast, c-A26/5FAM-Rev in the cell extract at ambient temperature responded to ATP with a K_D of 107 μM and revealed a relative fluorescent intensity change of more than 1.3-fold (Figure 6a); these values were comparable to those obtained under buffered conditions (Figure 2c). The slight increase in the K_D value of c-A26/5FAM-Rev to ATP in the cell extract may reflect that a small portion of RNP was degraded or that the sensing properties of the complex were affected by the factors in the cell media. A time course of changes in the fluorescence intensities of covalent and noncovalent sensors in the cell extracts was evaluated to assess the stability of the complexes (Figure 6b). Even after incubation for 120 min in the cell extract, c-A26/5FAM-Rev retained a sufficient response to ATP. These results indicated that the covalent linkage between the two subunits of the fluorescent RNP sensor enhanced the ability of the sensor to detect its target in cellular extracts at ambient temperature. The modification of the 3′-end of RNA would reduce the reactivity of 3′-*exo*-ribonucleases,[15] and the covalent linkage between the C-terminal of Rev and the 3′-end of RNA enhances the stability of Rev-RRE RNA, which in turn prevents the endonuclease reaction to some extent. The covalent modification thus converted the RNP sensor to a usable sensor for fluorescent sensing under physiological conditions.

CONCLUSION

Fluorescent sensors with optical characteristics tailored for given measurement conditions, such as the detection (or excitation) wavelength and ligand concentration range, are easily obtained from fluorescent ribonucleopeptide (RNP) libraries by taking advantage of the noncovalent properties of RNP complexes.[3a,d,e] The noncovalent configuration of the RNP needs an improvement for practical measurements, for instance, when one would like to reduce the sensor concentration or to apply multiple sensors in the same solution. For this purpose, formation of a covalent linkage between the ligand-binding RNA and the fluorophore-modified peptide provides a stable RNP sensor. Covalently linked RNP sensors showed enhanced thermostability and enabled the detection of ligands at lower concentrations of sensors, even in cell extracts.

Application of the covalently linked ATP and GTP sensors enabled the simultaneous real-time quantification of Ado and Ino in the reaction catalyzed by ADA. Each sensor responded exclusively to its ligand and permitted the simultaneous detection of changes in the concentration of ligands induced by an enzymatic reaction in the restricted concentration range. Because the combination of RNA and a fluorophore-modified peptide library afforded fluorescence responses in various concentration ranges, this strategy provided an appropriate set of fluorescent sensors for the detection of multiple ligands in the desired concentration range. Once a fluorescent RNP sensor with a desired property is obtained, the covalent linking strategy reported here allows development of fluorescent RNP sensors for simultaneous detection of multiple ligands by monitoring each wavelength corresponding to the respective ligand.

Unlike the RNA-based aptamer sensors, the covalently modified RNP sensors cannot be *in situ* generated inside the cell. However, the cell-permeable Rev peptide might be utilized to translocate the sensor into the cell. The covalently linked RNP sensors studied here show moderate relative fluorescence intensity changes of 1.2−3-fold upon binding the substrate. Because the fluorescent sensors with such moderate relative intensity changes were utilized as detection tools of signaling molecules in the cell,[16] further optimization in the response and stability of covalently linked RNP sensors would open their application in the cell.

MATERIALS AND METHODS

Pyrobest DNA polymerase for PCR reactions was obtained from TaKaRa Bio Inc. (Shiga, Japan), and the AmpliScribe T7 Kit for RNA preparation was from Epicentre (Madison, WI). *N*-α-Fmoc-protected amino acids, 2-(1*H*-benzotriazol-1-yl)-1,1,3,3-tetramethyluronium hexafluorophosphate (HBTU), 1-hydroxybenzotriazole (HOBt), *N*,*N*-diisopropylethylamine (DIEA), distilled *N*,*N*-dimethylformamide (DMF), diisopropylcarbodiimide (DIC), and *N*,*N*-dimethyl-4-aminopyridine (DMAP) were obtained from Watanabe Chemical Industries (Hiroshima, Japan). Dichloromethane (DCM) and HPLC-grade acetonitrile were purchased from Nacalai Tesque (Kyoto, Japan). 5-Carboxyfluorescein N-succinimidyl ester and 1-pyrenesulfonyl chloride were from Life technologies, Molecular Probes (Grand Island, NY). Cy5 mono NHS ester was from GE Healthcare Japan Inc. (Tokyo, Japan). 4-Hydroxymethylbenzoic acid PEGA resin (HMBA-PEGA resin) was from Merck, Novabiochem (Darmstadt, Germany). A reversed-phase C18 column (20 × 250 mm, Ultron VX Peptide; Shinwa Chemical Industries, Kyoto, Japan) and a RESOURCE-RPC column (3 mL, GE Healthcare) were used for purification of peptides for preparative purposes. Dulbecco's modified Eagle's medium (DMEM) was obtained from Sigma-Aldrich (St. Louis, MO). Trypsin was purchased from Life technologiesTM, Gibco (Grand Island, NY). Streptomycin was purchased from Meiji Seika Pharma, Co., Ltd. (Tokyo, Japan). Sodium periodate, hydrazine, gel electrophoresis grade acrylamide, bisacrylamide, phenol, thioanisol, 1,2-ethanditiol, and fetal bovine serum (FBS) were purchased from Wako Chemicals (Tokyo, Japan).

Construction of Noncovalent Fluorescent RNP Sensors. An RNA library was constructed with a randomized region containing up to 40 nucleotides adjacent to the RRE region and was added to the Rev peptide to afford an RNP library (RRENn RNP library), as described previously.[3e] ATP-binding RNP receptors were isolated from the RREN30 RNP library or the RRENn RNP library by in vitro selection as described.[3c,f] The nucleotide sequences used in this paper, except the RRE region, were as follows: A26, 5′-UUCCGGUAGUG-GUUGUGUGUGUGCGGUUUU-3′; G23, 5′-UGGAGCGGCUU-GUUGCGGAGUGUCUACUUG-3′; An16, 5′-CGUAGUGGUGU-GUGUGUGG-3′.[3c] For the conversion of RNP receptors to

dx.doi.org/10.1021/ja3097652 | J. Am. Chem. Soc. 2013, 135, 3465−3473

noncovalent fluorescent RNP sensors, the RNA subunit of the RNP receptor was combined with the fluorophore-modified Rev peptide to form a noncovalent complex.[3c]

Construction of a Stable Fluorescent RNP Sensor by the Covalent Linking Method. RNA subunits of RNP receptors were purified by denaturing 8% polyacrylamide gel electrophoresis. The purified RNA subunit was treated with freshly prepared sodium periodate to convert the cis-diol of the 3′-terminal ribose to 3′-dialdehyde by periodate oxidation.[12] Freshly prepared 50 equiv of 0.01 M sodium periodate (10 μL; 100 nmol) was added to 100 μM RNA (20 μL; 2 nmol) in 32 μL of 0.01 M sodium phosphate (pH 7.5), and the reaction mixture was incubated for 1 h at 37 °C in the dark. After the reaction, an excess of sodium periodate was reduced by adding glycerol (final concentration 1 M), and the resulting oxidized RNA was purified by ethanol precipitation.

The peptide subunit for the formation of a covalent linkage was synthesized by introducing a fluorophore to the N-terminus and the peptide linker (GGSGGSGGSG) with a hydrazide group at the C-terminus of the Rev peptide TRQARRNRRRRWRERQR GGSGGSGGSG. The modified peptide was synthesized as follows. A 4-hydroxymethylbenzoic acid PEGA resin (HMBA-PEGA resin; Novabiochem) was placed in a dry flask, and a sufficient amount of DMF was added to soak the resin; this mixture was allowed to swell for 30 min. N-α-Fmoc-glycine (10 equiv relative to resin loading) was dissolved in dry DCM with 1 or 2 drops of DMF and then mixed with a solution of DIC (5 equiv relative to resin loading) in dry DMF on ice. After incubating for 20 min, DCM was removed by evaporation under the reduced pressure. The residue was dissolved by minimum volume of DMF and added to the resin prepared above. A DMF solution of DMAP (0.1 equiv relative to resin loading) was added to the resin/amino acid mixture and incubated at room temperature for 1 h with occasional swirling. This first attachment procedure was repeated twice. The resin with the first amino acid was loaded onto an automated peptide synthesizer (PSSM-8; Shimadzu, Kyoto, Japan), and the subsequent synthesis was performed according to Fmoc chemistry protocols using protected Fmoc-amino acids and HBTU. A fluorophore with an activated group (5-carboxyfluorescein *N*-succinimidyl ester, 1-pyrenesulfonyl chloride, or Cy5 mono NHS ester) was directly coupled to the Fmoc-deprotected synthetic peptide on the resin. The fluorophore-labeled peptide was cleaved from the resin with 0.1 M hydrazine hydrate in DMF for 30 min at room temperature, washed with DMF, precipitated by ether, and then deprotected by a solution containing phenol (0.75 g), distilled water (0.5 mL), thioanisol (0.5 mL), 1,2-ethanditiol (0.25 mL), and TFA (10 mL) for 3 h. The N- and C-terminal modified peptide was gel filtrated with a G-10 resin, purified by reversed-phase HPLC, and characterized by MALDI-TOF mass spectrometry (AXIMA-LNR, Shimadzu) as follows: 5-carboxyfluorescein-modified Rev peptide hydrazide (5FAM-Rev-HZ), *m/z* 3471.8 (calcd for $[M+H]^+$ 3471.7); pyrene-modified Rev peptide hydrazide (Pyr-Rev-HZ), *m/z* 3376.1 (calcd for $[M+H]^+$ 3376.6); Cy5-modified Rev peptide hydrazide (Cy5-Rev-HZ), *m/z* 3747.3 (calcd for $[M+H]^+$ 3747.9).

A coupling reaction between the 3′-modified RNA (50 μM) and fluorophore-modified Rev-HZ (75 μM) was performed in 0.02 M sodium acetate (pH 5.2) containing 0.01 M NaCl (total 40 μL) at 37 °C in the dark. After 5 h, the reaction mixture was extracted by phenol-chloroform and then purified by ethanol precipitation. The precipitate was dissolved in 0.01 M sodium phosphate (pH 7.5) containing 0.1 M NaCl (40 μL). The sample solution was treated with a cation-exchange resin (SP Sepharose Fast Flow, GE Healthcare) for 30 min at ambient temperature to remove the excess peptide, and the unbound fraction was collected to obtain a covalently linked RNP complex. The sample solution was purified by 15% denaturing PAGE (6 M urea) and was subsequently quantified by measuring the absorption at 260 nm (A26 ε = 541 600 M^{-1} cm^{-1}, G23 ε = 538 000 M^{-1} cm^{-1}, An16 = 439 500 M^{-1} cm^{-1}). As a result, about 50 μL of 15 μM covalently linked RNP complex (c-A26/5FAM-Rev, c-G23/Pyr-Rev) was recovered (yield: 30−40%). c-An16/Cy5-Rev and c-G23/5FAM-Rev were prepared using the same procedure (yield: 75%).

MALDI-TOF MS Analysis of the Covalent RNP Complex. The covalently linked RNP complex was analyzed by a MALDI-TOF mass spectrometer (AXIMA-LNR, Shimadzu). A sample solution was desalted by a Sep-Pak C18 column (Waters), and a matrix solution was prepared with 0.07 M 3-hydroxypicolinic acid and 0.07 M diammonium hydrogen citrate in acetonitrile/H_2O (v/v: 1/1) for negative mode and with 2′,4′,6′-trihydroxyacetophenone monohydrate and diammonium hydrogen citrate in acetonitrile/H_2O/EtOH (v/v: 5/50/45) for positive mode. The sample solution was mixed with the matrix solution at a 1:1 (v:v) ratio on the MALDI sample plate and allowed to air-dry. Calibration of the instrument was carried out using oligodeoxynucleotides (molecular weights: 9145.8, 14 547.6, and 18 204.0) as external standard samples. Each mass spectrum was representative of an average of about 50 laser shots, and the laser power density was held constant at near threshold power density throughout these investigations. c-A26/5FAM-Rev: M^+ calcd 21557.3, found 21410.7; c-G23/Pyr-Rev: M^+ calcd 21507.4, found 21333.6 (Figure S9).

Fluorescence Measurements on the Microplate. Fluorescence measurements in 96-well plates were performed on a Wallac ARVOsx 1420 multilabel counter or Tecan Infinite M200 plate reader. A binding solution (100 μL) containing noncovalent or covalent fluorescent RNPs in 10 mM Tris-HCl (pH 7.6), 100 mM NaCl, 10 mM $MgCl_2$, and 0.005% Tween 20 with an indicated amount of substrate was gently swirled for a few minutes and allowed to sit for 30 min at the indicated temperature. Emission spectra were measured with an appropriate filter set for each fluorophore. Respective excitation and emission wavelengths were Pyr-Rev (350, 390 nm), 5FAM-Rev (485, 535 nm), and Cy5-Rev (650, 670 nm).

Determination of Ligand-Binding Affinity. The ligand-binding affinity of fluorescent RNP was calculated by fitting the ligand titration data using the following equation:

$$F_{obs} = F_{min} + A\{([FRNP]_T + [substrate]_T + K_D) - (([FRNP]_T + [substrate]_T + K_D)^2 - 4[FRNP]_T[substrate]_T)^{1/2}\}/2[FRNP]_T$$

where F_{obs} is the observed fluorescence intensity with each concentration of substrate, A is the increase in fluorescence at saturating substrate concentrations ($F_{max} - F_{min}$), K_D is the equilibrium dissociation constant, and $[FRNP]_T$ and $[substrate]_T$ are the total concentrations of fluorescent RNP and the substrate, respectively.

Simultaneous Detection of ATP and GTP in the Same Solution. Samples were prepared by mixing c-A26/5FAM-Rev (100 nM) and c-G23/Pyr-Rev (100 nM), or A26/5FAM-Rev (1000 nM) and G23/Pyr-Rev (1000 nM), and the indicated substrates in 10 mM Tris-HCl (pH 7.6), 100 mM NaCl, 10 mM $MgCl_2$, and 0.005% Tween 20. The samples were incubated for 30 min at 4 °C. When two noncovalent sensors were applied in the same solution, each noncovalent sensor was incubated in an independent tube for 30 min at 4 °C to secure the complex formation, then the solution containing the noncovalent sensor was added to the assay solution and incubated for 30 min at 4 °C. Fluorescence intensities were recorded on a Tecan Infinite M200 plate reader. The excitation wavelengths were 485 nm for 5FAM-Rev, 350 nm for Pyr-Rev, and 650 nm for Cy5-Rev. The emission wavelengths were 535 nm for 5FAM-Rev, 390 nm for Pyr-Rev, and 670 nm for Cy5-Rev and were used for the determination of relative fluorescence intensity.

Simultaneous Detection of a Substrate and a Product in an Enzymatic Reaction by Covalently Linked Fluorescent RNP Sensors. A sample was prepared by mixing c-A26/5FAM-Rev, c-G23/Pyr-Rev, and 100 μM Ado in 10 mM Tris-HCl (pH 7.6) containing 100 mM NaCl, 10 mM $MgCl_2$, and 0.005% Tween 20. The sample was incubated for 30 min at 15 °C, and then 0.1 mU of ADA was added to start the reaction. For the detection of changes in the concentrations of Ado and Ino, the fluorescence intensities were measured with Hitachi a F-4500 fluorescence spectrofluorophotometer with an excitation and emission bandwidth of 5 nm (ex.: 485 nm, em.: 535 nm for 5FAM-Rev; ex.: 350 nm, em.: 380 nm for Pyr-Rev) with

dx.doi.org/10.1021/ja3097652 | J. Am. Chem. Soc. 2013, 135, 3465−3473

reaction time. Amounts of the reacted substrate (Ado) and product (Ino) were converted using the standard curves calculated from the results of fluorescence spectroscopy of each substrate with the known concentration (Figure S8). The actual amounts of Ado and Ino with the reaction of ADA were measured by HPLC analysis for comparing to the results traced by the cRNP sensors (Figures 6b, S6, and S7).

Preparation of HeLa Cell Extracts. HeLa cells were seeded on 15-cm dishes and cultured in DMEM supplemented with 10% FBS, penicillin (30 units/mL), and streptomycin (30 μg/mL) at 37 °C in a humidified atmosphere consisting of 5% CO_2 and 95% air. After a 3-day culture, cells were harvested (total 2.5×10^8 cells). The pelleted cells were suspended in a binding buffer (10 mM sodium phosphate, pH 7.6, containing 100 mM NaCl, 10 mM $MgCl_2$, and 0.005% Tween 20) and sonicated for 10 min to obtain the cell lysate.[17] The efficiency of the cell homogenization was checked microscopically for cell lyses. The whole cell lysate was centrifuged at 12000*g* for 15 min. The supernatant was then passed through a 0.45 μm filter, and the protein concentration was measured by an RC DC protein assay kit (Bio-Rad, Hercules, CA). For a typical sample solution, the total protein of the supernatant was diluted to a final concentration of 1.0 mg/mL.

Titration Analysis of the RNP Sensors in HeLa Cell Extracts. Noncovalent A26/5FAM-Rev and covalent A26/5FAM-Rev (0.2 μM) were titrated with given concentrations of ATP in HeLa cell extracts. After 30, 60, or 120 min incubations, fluorescence measurements were performed in a Wallac ARVOsx 1420 multilabel counter (Perkin-Elmer) at 25 °C. Emission intensities were measured with a filter set for the fluorescein chromophore (ex.: 485 nm, em.: 535 nm).

■ ASSOCIATED CONTENT

Supporting Information

Structural models of covalent linking of the Rev-RRE complex (Figure S1), purity confirmation for the covalently linked RNP sensors (Figure S2), reaction of c-A26/5FAM-Rev under denature conditions (Figure S3), fluorescence titration analyses of c-An16/Cy5-Rev and c-G23/5FAM-Rev by ATP and GTP (Figure S4), saturation curves for the relative fluorescence intensity changes of c-A26/5FAM-Rev and A26/5FAM-Rev by titration with Ado (Figure S5), standard curves for the HPLC analysis of adenosine and inosine (Figure S6), time course profiles of the ADA reaction analyzed by HPLC (Figure S7), quantitative titration curves for fluorescent c-RNP sensors by adenosine and inosine (Figure S8), MALDI-TOF MS spectroscopy of c-RNP sensors (Figure S9), and chromatograms of reversed-phase HPLC analyses of c-RNP sensors (Figure S10). This material is available free of charge via the Internet at http://pubs.acs.org.

■ AUTHOR INFORMATION

Corresponding Author

t-morii@iae.kyoto-u.ac.jp

Notes

The authors declare no competing financial interest.

■ ACKNOWLEDGMENTS

This work was supported in part by a Grant-in-Aid for Scientific Research from the Ministry of Education, Culture, Sports, Science, and Technology, Japan to T.M. (No. 24121717).

■ REFERENCES

(1) (a) Weiss, S. *Science* **1999**, *283*, 1676−1683. (b) Zhang, J.; Campbell, R. E.; Ting, A. Y.; Tsien, R. Y. *Nat. Rev. Mol. Cell Biol.* **2002**, *3*, 906−918. (c) Giepmans, B. N.; Adams, S. R.; Ellisman, M. H.; Tsien, R. Y. *Science* **2006**, *312*, 217−224. (d) Wang, H.; Nakata, E.; Hamachi, I. *Chembiochem* **2009**, *10*, 2560−2577. (e) Tainaka, K.; Sakaguchi, R.; Hayashi, H.; Nakano, S.; Liew, F. F.; Morii, T. *Sensors* **2010**, *10*, 1355−1376.

(2) (a) Morii, T.; Sugimoto, K.; Makino, K.; Otsuka, M.; Imoto, K.; Mori, Y. *J. Am. Chem. Soc.* **2002**, *124*, 1139−1140. (b) de Lorimier, R. M.; Smith, J. J.; Dwyer, M. A.; Looger, L. L.; Sali, K. M.; Paavola, C. D.; Rizk, S. S.; Sadigov, S.; Conrad, D. W.; Loew, L.; Helinga, H. W. *Protein Sci.* **2002**, *11*, 2655−2675. (c) Toutchkine, A.; Kraynov, V.; Hahn, K. *J. Am. Chem. Soc.* **2003**, *125*, 4132−4145. (d) Nalbant, P.; Hodgson, L.; Kraynov, V.; Toutchkine, A.; Hahn, K. M. *Science* **2004**, *305*, 1615−1619. (e) Chan, P. H.; Liu, H. B.; Chen, Y. W.; Chan, K. C.; Tsang, C. W.; Leung, Y. C.; Wong, K. Y. *J. Am. Chem. Soc.* **2004**, *126*, 4074−4075. (f) Chan, P. H.; So, P. K.; Ma, D. L.; Zhao, Y.; Lai, T. S.; Chung, W. H.; Chan, K. C.; Yiu, K. F.; Chan, H. W.; Siu, F. M.; Tsang, C. W.; Leung, Y. C.; Wong, K. Y. *J. Am. Chem. Soc.* **2008**, *130*, 6351−6361. (g) Sakaguchi, R.; Endoh, T.; Yamamoto, S.; Tainaka, K.; Sugimoto, K.; Fujieda, N.; Kiyonaka, S.; Mori, Y.; Morii, T. *Bioorg. Med. Chem.* **2009**, *17*, 7381−7386. (h) Sakaguchi, R.; Tainaka, K.; Shimada, N.; Nakano, S.; Inoue, M.; Kiyonaka, S.; Mori, Y.; Morii, T. *Angew. Chem., Int. Ed.* **2010**, *49*, 2150−2153.

(3) (a) Morii, T.; Hagihara, M.; Sato, S.; Makino, K. *J. Am. Chem. Soc.* **2002**, *124*, 4617−4622. (b) Sato, S.; Fukuda, M.; Hagihara, M.; Tanabe, Y.; Ohkubo, K.; Morii, T. *J. Am. Chem. Soc.* **2005**, *127*, 30−31. (c) Hagihara, M.; Fukuda, M.; Hasegawa, T.; Morii, T. *J. Am. Chem. Soc.* **2006**, *128*, 12932−12940. (d) Hasegawa, T.; Hagihara, M.; Fukuda, M.; Morii, T. *Nucleosides Nucleotides Nucleic Acids* **2007**, *26*, 1277−1281. (e) Hasegawa, T.; Hagihara, M.; Fukuda, M.; Nakano, S.; Fujieda, N.; Morii, T. *J. Am. Chem. Soc.* **2008**, *130*, 8804−8812. (f) Nakano, S.; Mashima, T.; Matsugami, A.; Inoue, M.; Katahira, M.; Morii, T. *J. Am. Chem. Soc.* **2011**, *133*, 4567−4579. (g) Nakano, S.; Nakata, E.; Morii, T. *Bioorg. Med. Chem. Lett.* **2011**, *21*, 4503−4506. (h) Liew, F. F.; Hasegawa, T.; Fukuda, M.; Nakata, E.; Morii, T. *Bioorg. Med. Chem.* **2011**, *19*, 4473−4481. (i) Liew, F. F.; Hayashi, H.; Nakano, S.; Nakata, E.; Morii, T. *Bioorg. Med. Chem.* **2011**, *19*, 5771−5775.

(4) Battiste, J. L.; Mao, H.; Rao, N. S.; Tan, R.; Muhandiram, D. R.; Kay, L. E.; Frankel, A. D.; Williamson, J. R. *Science* **1996**, *273*, 1547−1551.

(5) (a) Ellington, A. D.; Szostak, J. W. *Nature* **1990**, *346*, 818−822. (b) Tuerk, C.; Gold, L. *Science* **1990**, *249*, 505−510.

(6) (a) Stojanovic, M. N.; de Prada, P.; Landry, D. W. *J. Am. Chem. Soc.* **2000**, *122*, 11547−11548. (b) Nutiu, R.; Li, Y. *J. Am. Chem. Soc.* **2003**, *125*, 4771−4778. (c) Nutiu, R.; Li, Y. *Angew. Chem., Int. Ed.* **2005**, *44*, 1061−1065. (d) Li, N.; Ho, C. M. *J. Am. Chem. Soc.* **2008**, *130*, 2380−2381.

(7) (a) Stojanovic, M. N.; Landry, D. W. *J. Am. Chem. Soc.* **2002**, *124*, 9678−9679. (b) Stojanovic, M. N.; Kolpashchikov, D. M. *J. Am. Chem. Soc.* **2004**, *126*, 9266−9270. (c) Jiang, Y.; Fang, X.; Bai, C. *Anal. Chem.* **2004**, *76*, 5230−5235. (d) Zhou, C.; Jiang, Y.; Hou, S.; Ma, B.; Fang, X.; Li, M. *Anal. Bioanal. Chem.* **2006**, *384*, 1175−1180. (e) Li, B. L.; Wei, H.; Dong, S. J. *Chem. Commun.* **2007**, 73−75.

(8) (a) Maynard, J.; Georgiou, G. *Annu. Rev. Biomed. Eng.* **2000**, *2*, 339−376. (b) Worn, A.; Plückthun, A. *J. Mol. Biol.* **2001**, *305*, 989−1010.

(9) Skerra, A.; Plückthun, A. *Science* **1988**, *240*, 1038−1041.

(10) (a) Glockshuber, R.; Malia, M.; Pfitzinger, I.; Plückthun, A. *Biochemistry* **1990**, *29*, 1362−1367. (b) Brinkmann, U.; Gallo, M.; Brinkmann, E.; Kunwar, S.; Pastan, I. *Proc. Natl. Acad. Sci. U.S.A.* **1993**, *90*, 547−551.

(11) (a) Bird, R. E.; Hardman, K. D.; Jacobson, J. W.; Johnson, S.; Kaufman, B. M.; Lee, S. M.; Lee, T.; Pope, S. H.; Riordan, G. S.; Whitlow, M. *Science* **1988**, *242*, 423−426. (b) Huston, J. S.; Levinson, D.; Mudgett-Hunter, M.; Tai, M. S.; Novotný, J.; Margolies, M. N.; Ridge, R. J.; Bruccoleri, R. E.; Haber, E.; Crea, R.; Oppermann, H. *Proc. Natl. Acad. Sci. U.S.A.* **1988**, *85*, 5879−5883.

(12) (a) Robberson, D. L.; Davidson, N. *Biochemistry* **1972**, *11*, 533−537. (b) Hansske, F.; Cramer, F. *Methods Enzymol.* **1979**, *59*, 172−181. (c) Proudnikov, D.; Mirzabekov, A. *Nucleic Acids Res.* **1996**, *24*, 4535−4542. (d) Cabezas, E.; Satterthwait, A. C. *J. Am. Chem. Soc.* **1999**, *121*, 3862−3875. (e) Kirchhoff, J. H.; Bräse, S.; Enders, D. *J.*

Comb. Chem. **2001**, *3*, 71−77. (f) Kozlov, I. A.; Melnyk, P. C.; Stromsborg, K. E.; Chee, M. S.; Barker, D. L.; Zhao, C. *Biopolymers* **2004**, *73*, 621−630. (g) Pfander, S.; Fiammengo, R.; Kirin, S. I.; Metzler-Nolte, N.; Jäschke, A. *Nucleic Acids Res.* **2007**, *35*, e25. (h) Sharon, J. L.; Puelo, D. A. *Biomaterials* **2008**, *29*, 3137−3142.

(13) (a) Heaphy, S.; Dingwall, C.; Ernberg, I.; Gait, M. J.; Green, S. M.; Karn, J.; Lowe, A. D.; Singh, M.; Skinner, M. A. *Cell* **1990**, *60*, 685−693. (b) Jain, C.; Belasco, J. G. *Cell* **1996**, *87*, 115−125. (c) Wang, Y.; Hamasaki, K.; Rando, R. R. *Biochemistry* **1997**, *36*, 768−779. (d) Kirk, S. R.; Luedtke, N. W.; Tor, Y. *J. Am. Chem. Soc.* **2000**, *122*, 980−981. (e) Zhang, C.-Y.; Johnson, L. W. *J. Am. Chem. Soc.* **2006**, *128*, 5324−5325.

(14) (a) Wolfenden, R.; Sharpless, T. K.; Allan, R. *J. Biol. Chem.* **1967**, *242*, 977−983. (b) Kati, W. M.; Acheson, S. A.; Wolfenden, R. *Biochemistry* **1992**, *31*, 7356−7366. (c) Ajloo, D.; Taghizadeh, E.; Saboury, A. A.; Bazyari, E.; Mahnam, K. *Int. J. Biol. Macromol.* **2008**, *43*, 151−158.

(15) (a) Osako, M. K.; Tomita, N.; Nakagami, H.; Kunugiza, Y.; Yoshino, M.; Yuyama, K.; Tomita, T.; Yoshikawa, H.; Ogihara, T.; Morishita, R. *J. Gene Med.* **2007**, *9*, 812−819. (b) Zhou, C.; Chattopadhyaya, J. *J. Org. Chem.* **2010**, *75*, 2341−2349. (c) Steen, K. A.; Malhotra, A.; Weeks, K. M. *J. Am. Chem. Soc.* **2010**, *132*, 9940−9943.

(16) (a) Namiki, S.; Sakamoto, H.; Iinuma, S.; Iino, M.; Hirose, K. *Eur. J. Neurosci.* **2007**, *25*, 2249−2259. (b) Tokunaga, T.; Namiki, S.; Yamada, K.; Imaishi, T.; Nonaka, H.; Hirose, K.; Sando, S. *J. Am. Chem. Soc.* **2012**, *134*, 9561−9564. (c) Kang, W. J.; Cho, Y. L.; Chae, J. R.; Lee, J. D.; Ali, B. A.; Al-Khedhairy, A. A.; Lee, C. H.; Kim, S. *Biomaterials* **2012**, *33*, 6430−6437. (d) Lee, M.-S.; Park, W.-S.; Kim, Y. H.; Ahn, W. G.; Kwon, S.-H.; Her, S. *Sensors* **2012**, *12*, 15628−15637.

(17) Endoh, T.; Funabashi, H.; Mie, M.; Kobatake, E. *Anal. Chem.* **2005**, *77*, 4308−4314.